

Mechanism of Graded Persistent Cellular Activity of Entorhinal Cortex Layer V Neurons

Erik Fransén,^{1,*} Babak Tahvildari,² Alexei V. Egorov,³ Michael E. Hasselmo,⁴ and Angel A. Alonso^{2,5}

¹School of Computer Science and Communication
Royal Institute of Technology
SE-100 44 Stockholm
Sweden

²Department of Neurology and Neurosurgery
Montreal Neurological Institute and
McGill University
Montreal, QC H3A-2B4
Canada

³Department of Neuroanatomy
Interdisciplinary Center for Neurosciences (IZN)
University of Heidelberg
Heidelberg D-69120
Germany

⁴Department of Psychology
Center for Memory and Brain
Boston University
Boston, Massachusetts 02215

Summary

Working memory is an emergent property of neuronal networks, but its cellular basis remains elusive. Recent data show that principal neurons of the entorhinal cortex display persistent firing at graded firing rates that can be shifted up or down in response to brief excitatory or inhibitory stimuli. Here, we present a model of a potential mechanism for graded firing. Our multi-compartmental model provides stable plateau firing generated by a nonspecific calcium-sensitive cationic (CAN) current. Sustained firing is insensitive to small variations in Ca^{2+} concentration in a neutral zone. However, both high and low Ca^{2+} levels alter firing rates. Specifically, increases in persistent firing rate are triggered only during high levels of calcium, while decreases in rate occur in the presence of low levels of calcium. The model is consistent with detailed experimental observations and provides a mechanism for maintenance of memory-related activity in individual neurons.

Introduction

Graded persistent spiking activity has been demonstrated in a variety of neural systems, such as the oculomotor system (Robinson, 1972), the somatosensory system (Romo et al., 1999), and the head direction system (Taube and Bassett, 2003), as recently reviewed (Frank and Brown, 2003; Major and Tank, 2004). It is not clear, however, whether the storage of graded information (the “memory” component of a neural integrator) relies primarily on synaptic dynamics or whether it may be endowed at the single-cell level. Our evidence of

intrinsic mechanisms for graded cellular spiking activity in entorhinal cortex (Egorov et al., 2002) and recently in lateral amygdala (A.V.E. et al., 2005, Soc. Neurosci., abstract 31, 612.11) indicates a significant role of autonomous cell behavior in graded persistent spiking. A fundamental question is therefore which mechanism, at the single-cell level, allows input integration and maintenance of graded levels of stable firing rate.

Any model must address the known experimental properties of graded persistent activity derived from analysis of previous data (Egorov et al., 2002). There are three basic characteristics of the process. First, a depolarizing pulse produces a brief high-frequency burst of spikes leading to an after-discharge that slowly drifts in frequency down toward a stable level (“persistent” level). Second, subsequent applications of the same stimulus lead to transient changes in frequency, each one of them quickly stabilizing at a gradually increasing level up to a point of saturation (≈ 12 Hz). Third, hyperpolarizing stimuli lead to transient decreases in firing frequency, each stabilizing at a lower level than the preceding one and eventually leading to cessation of firing. This persistent firing is activity dependent (i.e., Ca^{2+} dependent) and involves activation of a calcium-sensitive nonspecific cation current (CAN).

Other laboratories have provided models that have attempted to address how stable firing is achieved. Durstewitz (2003) proposed a scheme involving perfect balancing of currents across a range of membrane potentials. However, our new data (see Figure S1 in the Supplemental Data available online) suggest that blocking several conductances, such as the HCN or the A-current, does not affect stability (see “Experimental Observation” section), arguing that stable firing rates are not maintained purely through a delicate balancing of current conductance. Loewenstein and Sompolinsky (2003) presented an alternative model suggesting that persistent activity could be achieved by means of the propagation of a tonic Ca^{2+} wavefront along a dendrite. Similarly, Teramae and Fukai (2005) recently presented a model whereby firing rates were regulated in a manner involving Ca^{2+} release from stores. However, new data presented in this study indicate that the contribution of intracellular Ca^{2+} stores is not necessary to produce graded persistent activity in these neurons, thus potentially contradicting these two models. Moreover, as all of these models are based on line attractors, they are fundamentally unstable to noise or stimulus distractors and are therefore somewhat difficult to reconcile with experimental observations indicating that persistent firing is robust to distractors (i.e., brief depolarizing or hyperpolarizing current injections or synaptic inputs) and can occur under these conditions (Egorov et al., 2002).

The mechanism by which persistent firing is achieved appears to involve regulation of intracellular Ca^{2+} levels. Previous data showed that an intermediate (yet unknown) level of intracellular Ca^{2+} concentration, sustained by spiking, is required for the maintenance of a stable firing rate. Further, though measurements of intracellular Ca^{2+} concentration have not been performed

*Correspondence: erikf@nada.kth.se

⁵In memoriam, July 6, 2005

during persistent firing, previous data (Egorov et al., 2002) showed that positive shifts in the level of firing require beta frequency activation of the soma for 0.5–4 s (depending on the cell) and that negative shifts require robust somatic hyperpolarization for periods of typically 4 s or more. This suggests that crossing of a high level of $[Ca^{2+}]_{in}$ (an upper transition point) is required for the positive shifts, while crossing of a low level (going below a resting concentration) of $[Ca^{2+}]_{in}$ may be involved in the negative shifts. In entorhinal cortex layer V neurons, we have gathered evidence that biochemical signals may be involved in maintaining persistent firing (B.T. et al., 2004, Soc. Neurosci., abstract 30, 516.3). We propose that the Ca^{2+} -regulated cation channels that are involved in the process (Egorov et al., 2002) are under dynamic control by two competing processes, which for simplicity we have made analogous to phosphorylation and dephosphorylation and which stabilize a high and a low conductive state of the channel (Inoue et al., 1994; Walters et al., 1998). The model displays point attractor dynamics that are inherently stable, and it contains a mechanism for shifting the location of the stable point. The model reproduces all the experimental observations regarding graded firing in entorhinal neurons. Some of these data have been previously presented in abstract form (E.F. et al., 2004, Soc. Neurosci., abstract 29, 557.6; E.F. et al., 2003, Soc. Neurosci., abstract 30, 931.2).

Results

Experimental Observation

Figure 1A shows new data replicating the previously presented up- and downward regulation of “persistent” graded firing in an entorhinal cortex (EC) layer V neuron in response to depolarizing and hyperpolarizing inputs, respectively (Egorov et al., 2002). Using multiple different transitions to enter a range of different graded states (Figures 1B1 and 1B2), we show that graded firing in these cells is not discrete but can exist along a continuum within a restricted range of frequencies (for graded levels between 3 Hz and 12 Hz). Analyses show that persistent firing is truly stable for very prolonged periods of time, as demonstrated by the perfect linearity of the cumulative interspike interval analyzed for experimental data during a “persistent” state (Figures 1C1 and 1C2).

Recent models propose that Ca^{2+} waves could create a dendritic Ca^{2+} front with an activity-dependent location that would thereby define graded levels of firing through a read-out process by a CAN current (Loewenstein and Sompolinsky, 2003) or that nonlinear interaction with internal stores could store graded levels (Tera-mae and Fukai, 2005). To test these hypotheses, we reduced intracellular calcium stores by either blocking of Ca^{2+} -ATPase with cyclopiazonic acid (CPA) (50 μ M, $n = 10$, Figure 2) or by depleting ER calcium with application of thapsigargin (1 μ M, $n = 3$, data not shown). Neither the application of CPA nor thapsigargin resulted in a disruption in the ability of the EC layer V cells to generate graded persistent firing. CPA was effective as indicated by the separate reduction of the AHP. An alternative model, proposed by Durstewitz (2003), suggested that persistent firing resulted from the balancing of currents across a range of membrane potentials. To test

this model, we blocked several conductances, such as the HCN (CsCl at 5 mM, $n = 3$, Figure S1A2) or the potassium A-current (4-aminopyridine at 5 mM, $n = 4$, Figure S1B2). Blocking these currents did not interfere with stability, suggesting that stable graded activity does not depend on a delicate balance of currents.

System Conditions

Using both prior existing biological data and our new experimental results, we evaluated different dynamical systems that may provide all of the required properties, as represented diagrammatically in Figure 3. Each system strives to attain the nearest lowest point on the y axis while influenced by the control parameter (increasing direction indicated by arrow; in our case indicating calcium concentration $[Ca^{2+}]_{in}$ which gates a CAN current). Case A corresponds to a fixed-point attractor with a single stable level and thus cannot explain our system. Case B corresponds to a line attractor. It has an arbitrary number of levels (graded system), none of which are stable, and thus cannot correspond to our system either. Case C represents a system with potentially a large number of fixed points. This scenario has restrictions on how many stable points may exist while the system maintains tolerance to noise and distractors and is thus not consistent with the new data in Figure 1B2. In addition, this multistable system would not show a stereotyped transient decay to a new level as observed experimentally (Figure 1A). We therefore considered as most likely the scenario represented in panel D; the case of a point attractor with a location that can be continuously shifted along a range of values.

The next issue is how the point attractor may be moved to a new level. Experiments indicate that induction of a new level involves a threshold, as a minimal time and amplitude of stimulation are necessary to change the stable firing rate, Figures 5C and 5D (see Egorov et al., 2002; Figures 1B and 1C). The robustness to noise and distractor inputs (Egorov et al., 2002) also suggests the presence of a threshold to achieve state changes. With regard to thresholds, Figure 3E shows that a system displaying only one fixed threshold is a bistable system, which is not our case. With many thresholds (Figure 3F), a system could reach many levels, but the biochemical implementation of such a system is very unclear. If a single threshold could be moved, as in Figure 3G, there could be multiple levels, but the biochemical implementation of this is also unclear, as the threshold would have to be moved along with the change in firing level. However, in a system that includes upper and lower thresholds as transition points and a neutral region in between, as in the scenario depicted in Figure 3H, multiple stable levels are easily obtained, and the system provides noise and distractor tolerance as well as transitions both up and down.

In summary, our hypothesis involves a mechanism of stability and a mechanism of change. The mechanism of stability involves a stable balance between depolarizing currents (e.g., the CAN current) and hyperpolarizing currents (currents involved in membrane resting potential and AHP). The mechanism of change involves two transition points of calcium concentration, an upper transition point leading to increases in CAN current and a lower transition point leading to decreases, both due to Ca^{2+} -dependent metabolic processes. Between these

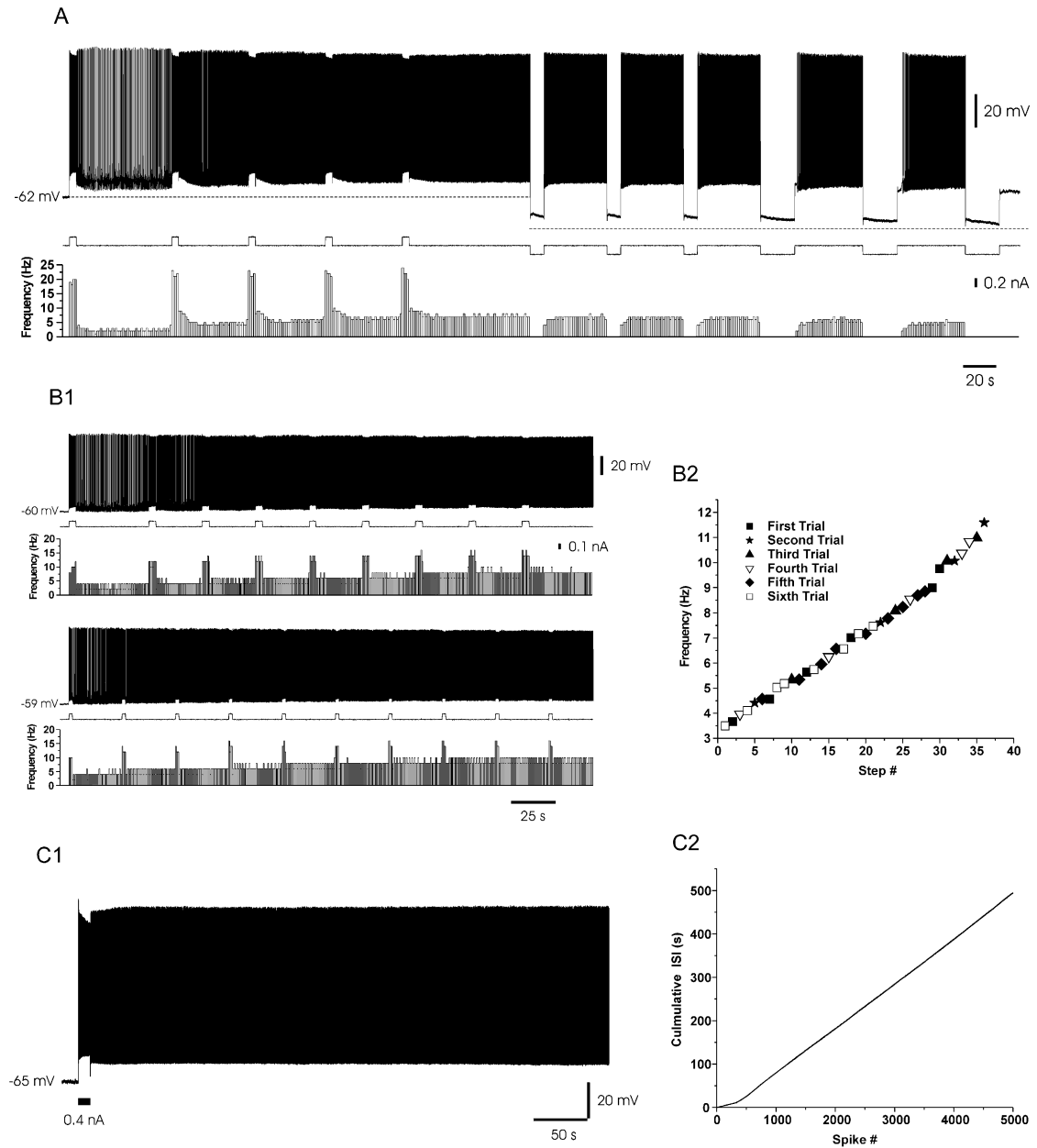


Figure 1. Stable Graded Spiking

(A) Up- and downregulation of neuronal firing frequency. The figure shows an experiment with ten different stable levels induced by five depolarizing followed by six hyperpolarizing current injections. Top, soma membrane potential; middle, current injection; bottom, spike frequency histogram. (B) Continuum of levels. (B1) Experimental data from one cell, showing changes in firing frequency during two sequences of repeated depolarizing current injections. (B2) Experimental data from one cell, showing a continuum of stable graded levels entered at different times over six consecutive trials (two of them shown in [B1]). Note the proximity between stable levels, in a total of 36 observations for this cell, and the absence of stepwise changes in frequency. Steps were sorted based on frequency; different symbols correspond to different series of step depolarizations. Similar multilevel stability has been observed in all cases tested ($n = 8$). (C) Stability of firing at plateau. (C1) Experimental recording of soma membrane potential over a 7.5 min stable plateau containing over 5000 spikes. (C2) Cumulative interspike interval (ISI) plot of the same cell. Note the linear increase indicating a very stable firing frequency. Firing frequency was 9.8 Hz. The initial smaller slope comes from the stimulation period with a frequency of about 30 Hz.

transition points there is a neutral region where the metabolic processes are balanced. The neutral region provides stability to noise and distractors. As transition points are located outside the calcium range occupied by stable graded levels, graded levels are not subject to positive feedback and related problems of runaway activity.

Implementation

Because experimental data indicate involvement of Ca^{2+} -dependent regulation of a CAN current, the hypothesis shown in Figure 3H was simulated using changes in the conductance of single CAN channels, as described in Figures 4A–4D and Experimental Procedures. We propose that individual CAN channels can

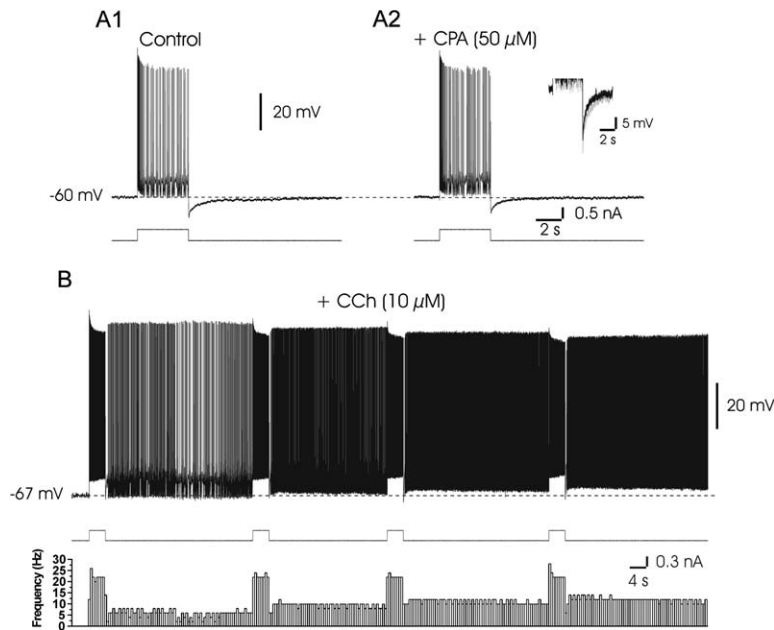


Figure 2. Graded Persistent Activity Does Not Depend on Intracellular Ca^{2+} Stores

Depletion of intracellular Ca^{2+} stores with cyclopiazonic acid (CPA) did not prevent the neurons' ability to generate graded persistent activity. (A1 and A2) Firing behavior (upper traces) of a layer V EC neuron to step depolarization current pulse (lower traces) in control and after perfusion with CPA (50 μM for 30 min), respectively. (Inset in [A2]) Membrane potential traces of (A1) and (A2) superimposed at larger time and voltage scales. Action potentials are truncated. Trace in black belongs to CPA application. Note the reduction of the peak of AHP which was observed in all five tested neurons. (B) Graded persistent activity observed in the same neuron as in (A) following superfusion with CCh (10 μM).

exist in two states: a high conductive state reached in a probabilistic manner when Ca^{2+} rises above a higher transition point, and a low conductive state to which channels shift in a probabilistic manner when Ca^{2+} falls below a distinct lower transition point. Between the two transition points, the state of the CAN channels remains stationary. The changes in CAN channel could be mediated by one of many Ca^{2+} -dependent biochemical processes. Here we attribute the changes to phosphorylation/dephosphorylation, as shown in Figure 4A, which starts with a high threshold Ca^{2+} current and ends with a CAN current up- or downregulated by phosphorylation or dephosphorylation. The phosphorylation pathway favoring the high state (H) is denoted P and the dephosphorylation pathway favoring the low conductance state (L) is denoted D. In Figure 4B, the curves indicate the transition probability, which is a continuous entity although individual channels behave in a binary manner. When the number of channels is large, the macroscopic transitions appear graded (Lisman and Goldring, 1988). For a single Ca^{2+} point on the x axis, the population of channels will be split between a subset on the upper curve (dotted line) and a set on the lower curve (along the x axis), resulting in a graded level of total conductance. The model balances all transmembrane currents at each stable level according to the hypothesis in Figure 3D. Membrane potential and calcium level interact via calcium channels and calcium-dependent channels [e.g., K(AHP) and CAN channels]. At a stable level, voltage- and calcium-dependent currents are in balance. Any deviation from a stable point will correspond to a change in a 3D space of I , V_m , and $[\text{Ca}^{2+}]$, as shown in Figure 4C. For clarity, Figure 4D shows the phase plane of calcium dependence and not voltage dependence (see Experimental Procedures). The compound current resulting from Ca^{2+} -activated K channels and voltage-gated Ca^{2+} channels and several states of CAN current activation are plotted. For example, when 50% of the CAN channels are in the high conductance

state, there is a Ca^{2+} level Ca_{T50} below which the cell is stable at resting potential and above which the cell is stable at the point Ca_{S50} (stable plateau point at the intersection of the balancing currents). Note that the curve of transition probabilities for L-H in Figure 4B is primarily at higher Ca^{2+} concentrations than the stable point S50 in Figure 4D. For increasing or decreasing numbers of CAN channels in a high state, the stability point moves, respectively, to higher or lower Ca^{2+} and membrane potential levels. For technical reasons, we have not experimentally quantified intracellular Ca^{2+} concentration during stable firing levels, but experimental observations indicate that V_m changes in a stable manner in correlation with each firing level (Figure 1A). If a change in Ca^{2+} occurs, but this change is within the neutral region between the upper and lower transition points (see Figure 4B), then there is no change in the state of the CAN channels and the cell returns to the stability point at the end of the perturbation. If the curve of I_{CAN} is below that of $I_{\text{K(AHP)}}$ for all values, there is no stable spiking. Also, for high percentages of high conductance states and high levels of $[\text{Ca}^{2+}]$, there may be no region where $I_{\text{K(AHP)}}$ exceeds I_{CAN} , resulting in spiking activity going to the maximal (saturated) level of firing.

Testing the Model

The above scheme was tested in a multicompartmental model of an EC layer V principal cell as described in Experimental Procedures. We first tested whether the model would respond to input with plateau potentials with characteristics corresponding to experiments. As illustrated in Figures 5A and 5B, plateau duration changed as a function of stimulus magnitude and duration according to the same profile as found in the experiments (Figures 5C and 5D). The model cell also displayed a threshold (minimal amplitude and duration of input) for induction of a persistent stable level, in agreement with the experimental observations (Egorov et al., 2002, Figures 1B and 1C). In Figure 5E, we show the ability to

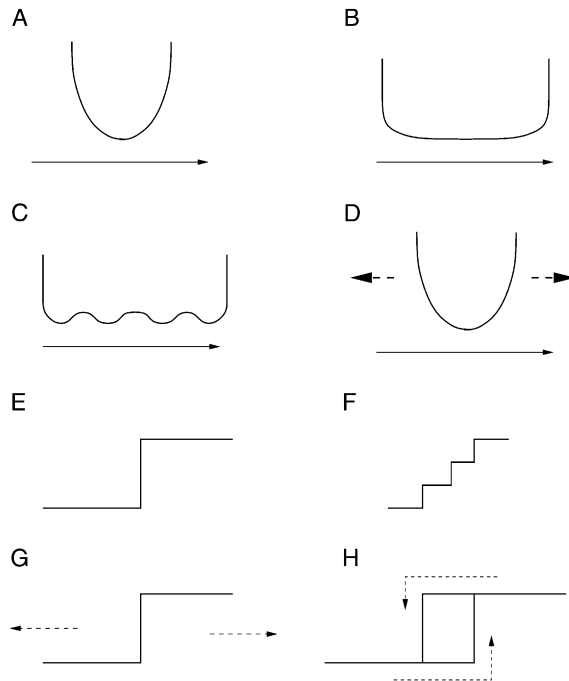


Figure 3. Principles of Stability and Induction

(A–D) Stability dynamics of model. Arrow indicates direction of increasing control parameter, i.e., membrane potential or calcium concentration. The system is assumed to attain the lowest point on the curve as seen in a local neighborhood. Thus, vertical axis represents, e.g., net current per unit calcium, so that positive slopes indicate a net excess of hyperpolarizing current. (A) Fixed-point attractor. Only one stable value, but displays stability to noise. (B) Line attractor. Infinite number of values, but unstable to noise. (C) Multiple fixed-point attractors. Multiple stable values that are stable to noise, but discretely spaced. (D) Movable fixed-point attractor. The position of the point of stability can attain an arbitrary value, thus giving an infinite number of stable values that are stable to noise.

(E–H) Induction of stable levels. (E) One fixed threshold. This provides only two stable levels and the point of transition from one to the other is the same. (F) Multiple thresholds. The biochemical implementation of multiple stable points seems unclear and probably requires a complex biochemical network. As in (E), the transition points are the same going up and down. (G) Movable fixed threshold. This produces an arbitrary number of stable levels, but as in (F), the biochemical implementation is unclear and presumably complex; and as in (E) and (F), transitions points up and down are the same. (H) Separate thresholds. With separate transition points for up and down transitions, the system possesses hysteresis. With a neutral region, it can attain graded levels, as one fraction of the system can be maintained in the upper region at the same time as the other fraction is maintained at the lower level.

generate a continuum of graded levels, corresponding to the experimental data shown in Figure 1B1. In Figure 5F, the stability of the firing is shown for data from a 6 min simulation comprising more than 3200 spikes, to be compared to the experimental data in Figure 1C2.

We subsequently tested the ability of the model cell to reproduce the firing behavior seen in experiments when a sequence of depolarizing and hyperpolarizing inputs is applied (as in Figure 1A). This is illustrated in Figure 6 along with the computed changes in $[Ca^{2+}]_{in}$ and G_{CAN} . The model reproduces the range of stable graded levels shown in experiments with a lowest level at 3 Hz and a highest level at 12 Hz. First, note that during the second depolarizing input firing frequency accelerates (1). Sec-

ond, and very importantly, there is then a period of transient decay in frequency (2) until a steady-state level is reached (i.e., the stable firing level is not attained immediately). Third, when a subsequent depolarizing input is applied, the same pattern is observed, and at the end of the input, frequency again decreases to a new steady level higher than the previous one (3). This is fully consistent with what is observed experimentally. Fourth, if a hyperpolarizing input is applied (4), V_m monotonically decays during the input as observed experimentally (Figure 1A), consistent with the notion of turning off an inward current. Fifth, after the end of the hyperpolarizing pulse (5), firing starts slow and there is a transient increase in firing frequency until a new steady level is reached, which is lower than the preceding one. Sixth, the model is stable to depolarizing and hyperpolarizing distractors (6) (very brief current injections that appear as upward and downward lines in the figure). Finally, a repetition of the longer hyperpolarizing current injection decreases firing further (7), and another repetition then stops the activity (8). The model replicates the full range of graded plateaus from 3 to 12 Hz (see Figure 5E), as found in experiments. Thus the model is able to reproduce the characteristics of graded persistent firing in its finest details.

To better demonstrate the dynamics of the process, phase plane plots of the variables of the system during a transition to a new stable level are presented in Figure 7. Panel 7A depicts $[Ca^{2+}]_{in}$ as a function of V_m , and panel 7B plots G_{CAN} as a function of $[Ca^{2+}]_{in}$ for the time interval 22–43 s of Figure 6 (upward transition around [C]). Note that since the CAN current is directly gated by Ca^{2+} , it increases rapidly during stimulation. This does not, however, lead to a rapid increase in the number of channels in the high conductive state as can be seen in the phase plane plot for the activation of H_{CAN} as a function of $[Ca^{2+}]_{in}$ (panel D). This change occurs with a delay, as the internal calcium first must reach the upper transition point for transitions and then is limited by the kinetics of the metabolic pathway (Figure 4A). Similarly, during a downward transition, Figure 7C (time interval 46–68 of Figure 6 around [D]) the decreased level of Ca^{2+} rapidly affects G_{CAN} without an immediate decrease in the number of channels in the high conductance state. This process similarly takes longer, as the internal calcium first must decay to the lower transition point and then is limited by the kinetics of the metabolic path. The kinetics of the metabolic process are thus essential to provide the system with robustness to noise and distracting stimuli and to prevent slow drifting from the initial steady level. The model described above was also subjected to a number of tests to assess sensitivity to noise and parameter variation, see Supplemental Methods section “Model tests and sensitivity analysis.”

Discussion

These results address how neurons can generate stable graded changes in activity that are of fundamental use in working memory. This single-cell model reproduces properties of intrinsic persistent spiking that EC layer V neurons can develop during cholinergic muscarinic modulation. Our model predicts that graded changes in firing frequency can be obtained with a Ca^{2+} -regulated

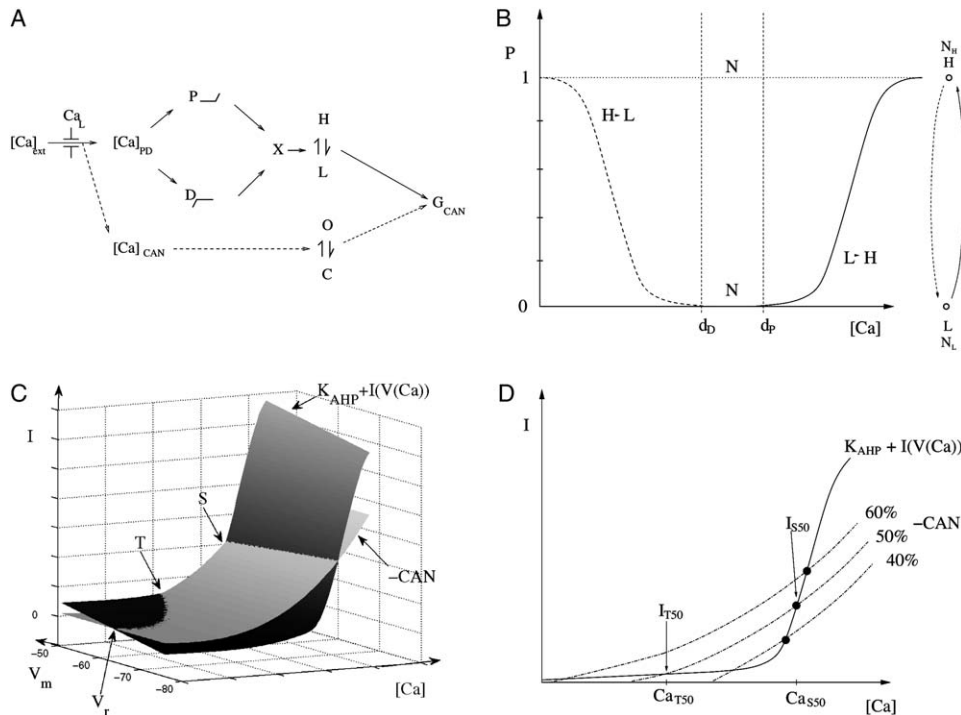


Figure 4. Implementation of Stability and Induction

(A) Biochemical pathway. Schematic model signaling network. Influx of calcium via a high-threshold calcium channel Ca_L affects the CAN current conductance G_{CAN} both directly (dashed pathway, direct regulation of balance between open state O and closed state C) and indirectly via the phosphorylation-dephosphorylation pathway (solid arrow to $[Ca]_{PD}$). Phosphorylation (P) and dephosphorylation (D) affect the regulatory product X, which influences the balance of CAN channels between the high conductance state (H) and the low conductance state (L), respectively. (B) Model of stability and change of level. Single-channel transition probabilities dependent on concentration of calcium. The y axis P plots the probability of the channel to change state. Solid line (labeled L-H) shows transition probability to change from low to high conductance state. Dashed line (H-L) shows transition probability to change from high to low. Both transitions depend on intracellular calcium concentration (or an interrelated product). During stable states, calcium stays within N, the neutral concentration region and channels remain in their respective state. (Right) Arrows, single-channel state transitions. L, low conductance state; H, high conductance state. N_x , number of channels in each respective state. (C) 3D plot showing planes representing the amount of current (I) through the CAN channel ($-CAN$) and the K(AHP) channel ($K_{AHP} + I(V(Ca^{2+}))$, including voltage-dependent channels), for different values of calcium concentration (x axis) and membrane potential (y axis). Stable graded levels of firing lie on the intersection of these two curves labeled "S." Unstable points, above which CAN dominates, are labeled "T." Below T, $K_{AHP} + I(V(Ca^{2+}))$ dominates, bringing the cell to resting membrane potential, V_r . (D) Balancing currents. The magnitude (I) of the two opposing calcium-dependent currents CAN (dot-dash line) and K_{AHP} (solid line) are plotted across a range of calcium concentrations (note that the range is lower than in (B)). The intersection points (filled circles) symbolize three levels of stable firing, all of which fall within the neutral region in (B). Percentages indicate the proportion of high conductance channels of I_{CAN} . Ca_{S50} indicates the stable level for 50% high conductance channels, and Ca_{T50} indicates an unstable point. Potentials below resting potential are omitted for simplicity.

metabolic cascade that acts in a push-pull fashion via, e.g., kinases/phosphatases on total CAN channel conductance. The model also predicts that there must be two separate Ca^{2+} transition points for the metabolic cascade, with a neutral region in between. The plausibility of these predictions are discussed below. Our model avoids problems of stability (drifting) associated with other models using line attractor approaches. Recent experimental evidence for graded persistent activity in lateral amygdala (A.V.E. et al., 2005, Soc. Neurosci., abstract 31, 612.11) suggests that this phenomenon may be of general function.

The problem of maintaining stability for prolonged periods of time is a general problem of homeostatic regulation of cellular function that is universally solved through metabolic processes. The role of biochemical signals in graded firing is supported by data showing that the phenomenon washes-out rapidly during whole-cell patch-

clamp recording (B.T. et al., 2004, Soc. Neurosci., abstract 30, 516.3). This model is just a minimal example of a sufficient metabolic system. Our scheme could be implemented in a number of different ways. However, because of the generality of phosphorylation, we suggest this mechanism increases the Ca^{2+} sensitivity of the I_{CAN} current and/or channel open time (Inoue et al., 1994; Walters et al., 1998), and several factors have been shown to modulate CAN channels, e.g., lipid messengers like DAG and PIP_2 . A key factor is that the calcium concentration must cross above or below the transition points for de/phosphorylation to occur. This provides the robustness to noise, prevents drifting, and prevents positive feedback from leading to saturated firing frequency or termination of firing. Two different transition points for opposing processes separated by a neutral region have been reported for the induction of long-term potentiation and depression of synaptic

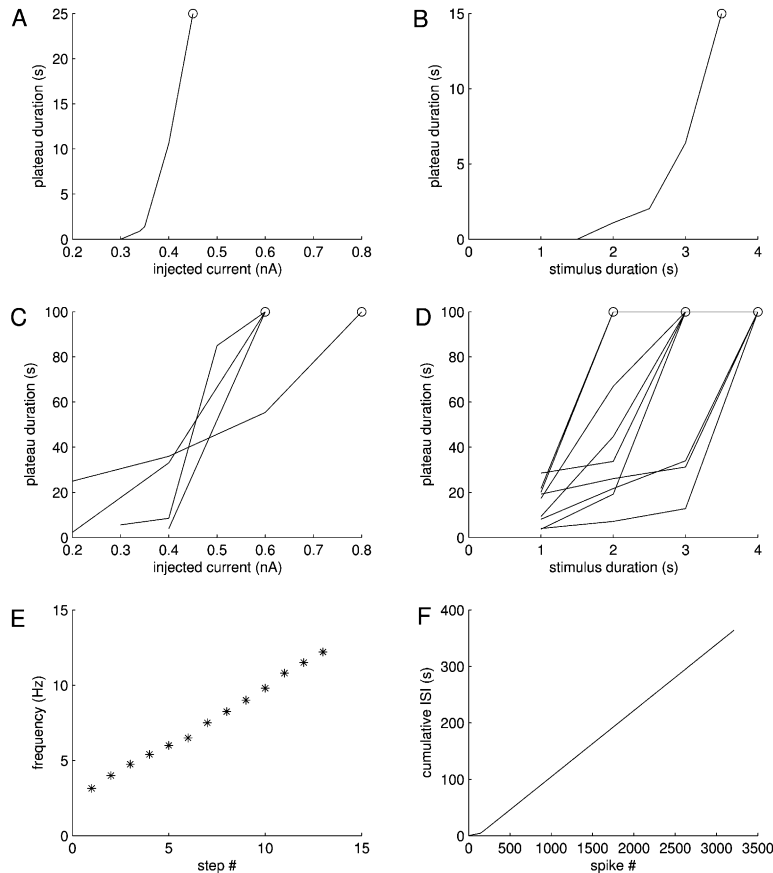


Figure 5. Plateau Duration

The plateau duration depends on stimulation time and magnitude.

(A and B) Simulation results showing plateau duration dependent on magnitude (A) or duration (B) of injected current that triggers the plateau; for (A), current injection duration was 2 s; for (B), current injection amplitude was 0.48 nA. Circled point at top of each plot represents the values for which a stable persistent plateau was obtained (i.e., duration was beyond the range of the plot on the y axis). Other points represent shorter transient plateaus with duration shown on y axis. Note that in all cases there is a lower point below which no plateau is present. Time in seconds. (C and D) Experimental data. Multiple curves indicate data from different cells. Units are nA and seconds. For (C), current injection durations were between 1.0 and 4.0 s. For (D), current injection amplitudes were between 0.2 and 0.6 nA.

(A and C) Plateau duration depends on the magnitude of injected current.

(B and D) Plateau duration depends on the duration of injected current.

(E) Continuum of levels. Simulation data of the frequency during plateaus after 13 different depolarizing current injections, similar to Figure 1B2.

(F) Stability of firing at plateau. Cumulative interspike interval (ISI) plot for a simulation of 6 min plateau activity, similar to Figure 1C2. Firing frequency was 8.6 Hz. The initial smaller slope comes from the stimulation period with a frequency of about 30 Hz.

transmission at higher and lower levels of calcium, respectively (Cho et al., 2001), see also the discussion of “no man’s land” by Lisman (2001). Further, dynamical control by calcium-dependent kinases and phosphatases has been shown to be essential for working memory function (Runyan et al., 2005).

Intracellular biochemical reactions under well-mixed conditions with line attractor dynamics can represent a continuum of levels (Lisman, 1994; H. Malmgren, Fifth International Conference on Cognitive and Neural Systems, abstract, Boston, 2001), but such a system would not possess robustness to noise or distractors. Noise would generate a random walk, and the system would lose its memory at the rate of this diffusion. A line attractor in its pure form will therefore only work in mathematically ideal systems and not in a living cell. Further, for time periods that are moderately long, diffusion systems have been constructed that can store a graded level that depends on the amplitude of the input (Okamoto and Ichikawa, 1994). Such a model does not, however, have a threshold for the input and will thus be sensitive to distractors. If the system possesses hysteresis (Koullakov et al., 2002; Loewenstein and Sompolinsky 2003), this can provide some level of stability to this inherent instability of a line attractor mechanism. The biochemical implementation of such an alternate mechanism for hysteresis still has to be specified.

Our model differs fundamentally from models related to line attractors. We have separated mechanisms for changing the stable level (conductance state changes) from mechanisms providing stability of the level (the bal-

ance between CAN and K-currents). Thereby the problems of stability are avoided while providing a means of graded change. If in our model I_{CAN} and $I_{K(AHP)}$ were coigned (by slanting and bending of either activation curve), the mechanism suggested by Durstewitz (2003), a line attractor is possible. However, stability is lost as the restoring current [the difference between I_{CAN} and $I_{K(AHP)}$] vanishes. For weak restoring currents, one would observe large-amplitude oscillations around a central point, something not observed experimentally (see Figures 1C1 and 1C2). A delicate balance across a voltage range is further not consistent with our experimental results that blocking conductances such as the HCN or the potassium A-current does not affect stability.

A switch-like activation of principal dendrites (Heckman et al., 2003) was suggested by Connors (2002) to account for the cellular stable graded levels discussed in the present work. Such a model would give the neuron a discrete number of stable levels, as it has dendritic compartments and thus a limited number of activity levels. One would also expect to see activation of parts of the dendrite at a time and, thus, a stereotyped pattern of stepwise changes of levels. This is inconsistent with experimental data in Figures 1B1 and 1B2 showing how a cell can have many closely spaced stable levels, indicating a continuum of stable levels and no apparent discretization. Additional modeling shows that our results do not depend critically on whether localization of the CAN channel and its associated signaling pathway is somatic or dendritic (dendritic modeling not shown).

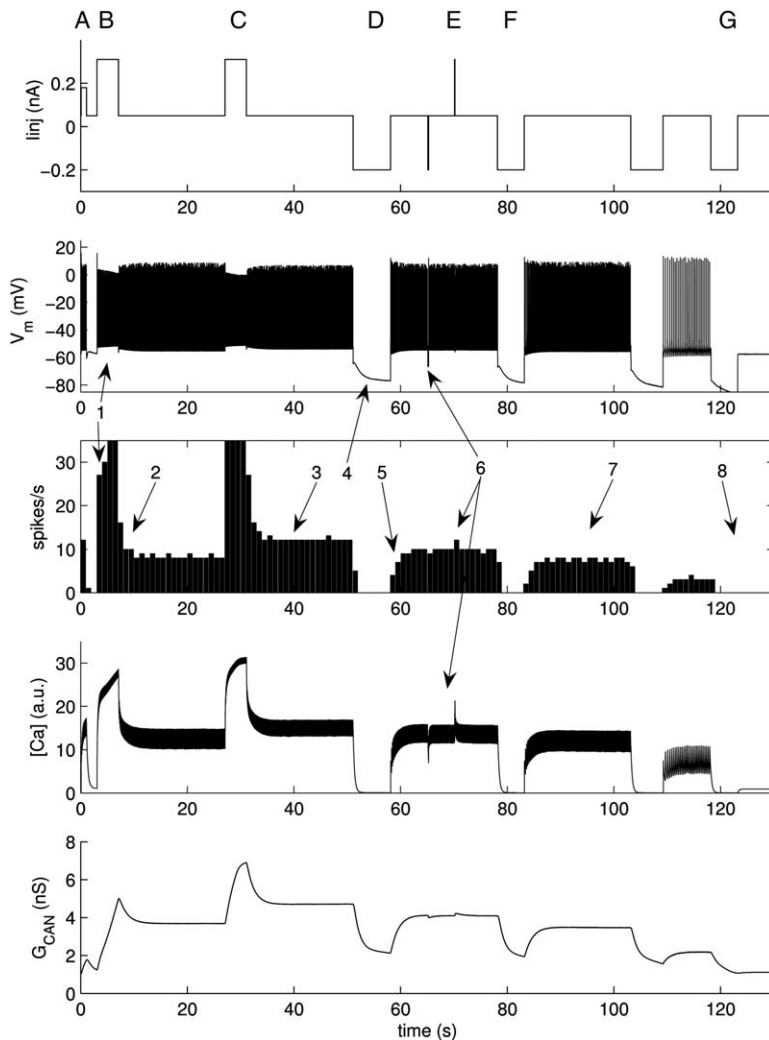


Figure 6. Stable Levels of Model

The simulation shows the properties of experimental data shown in Figure 1. In the figure we plot from top: the current injection I_{inj} (nA), soma membrane potential V_m (mV), spike histogram (bin width 1s), calcium concentration (arbitrary units), and cationic current conductance G_{CAN} (nS). Starting from left, at (A) the neuron responds to a weak current injection (0–2 s) with spiking during injection alone. Next (B), a larger magnitude depolarization (at time 3–7 s) causes a firing increase followed by transient decay to a stable firing frequency. This stable firing persists until another depolarizing injection (C) at time 27–31 s. Firing increases during injection and decays to a higher graded level. At 51–58 s (D), a hyperpolarizing injection prevents firing during injection, but after injection the firing rate transiently increases to a lower graded level. Very brief distractor injections (E) (hyperpolarizing at 65 s and depolarizing at 70 s) do not alter this frequency. At 78 and 101 s (F), more hyperpolarizing injections shift the stable state to subsequent lower frequencies, and at 118 s (G), a final hyperpolarizing current injection terminates the stable firing.

The proposed mechanism does not therefore depend on a specific spatial location or spatial distribution.

Using multicompartamental representation of dendritic branches containing voltage-dependent Ca^{2+} channels, Loewenstein and Sompolinsky (2003) have produced multiple stable graded levels of firing of an isolated neuron. The model builds on Ca^{2+} diffusion between well-defined calcium sources and sinks. The function thus relies on the presence of stable and continuous calcium concentration fluxes over the entire stable period. As discussed by Wang and Major (2003), the major drawback is how this mechanism could be implemented with known properties of calcium release, buffering, and extrusion. Specifically they bring up features like Ca^{2+} inactivation and diffusion of the receptor, disturbing the stability of the Ca^{2+} fronts. As they note, most of these components show desensitization or inactivation, effectively opposing the stability of the suggested model. Our experimental results excluding interaction with internal calcium stores or IP_3 pathways further argue against this approach. Thus, albeit this model fulfills the functional requirements of multiple stable graded levels and shows tolerance to noise, its central assumptions of continuous calcium and calcium-related product flux are not supported experimentally.

Previous simulations of mechanisms for sustained spiking in the absence of input have focused to a large extent on obtaining binary on or off states of spiking activity typical of fixed-point attractors (e.g., Fransén and Lansner, 1995, 1998; Amit and Brunel, 1997; Camperi and Wang, 1998). Most of these models of the maintenance of sustained activity have focused on the role of synaptic recurrent connections.

As an alternative or complement to recurrent synapses, intrinsic Ca^{2+} -dependent cation currents have also been proposed to underlie sustained spiking with binary properties (Lisman and Idiart, 1995; Fransén et al., 2002; Koene et al., 2003). Indeed, experimental data on a cationic current producing plateau-type firing (Klink and Alonso, 1997; Shalinsky et al., 2002) support this hypothesis of an intrinsic mechanism.

The present work concerns the case of graded spiking activity levels. Our data show how a single neuron in the absence of synaptic input can sustain stable graded firing. Other models of graded activity, however, build on interactions in a network (Cannon et al., 1983; Amit and Brunel, 1997; Seung et al., 2000; Compte et al., 2000; M. Goldman et al., 2002, Soc. Neurosci., abstract; Koulakov et al., 2002; Brody et al., 2003; Miller et al., 2003). Experimental data do not rule out the possibility

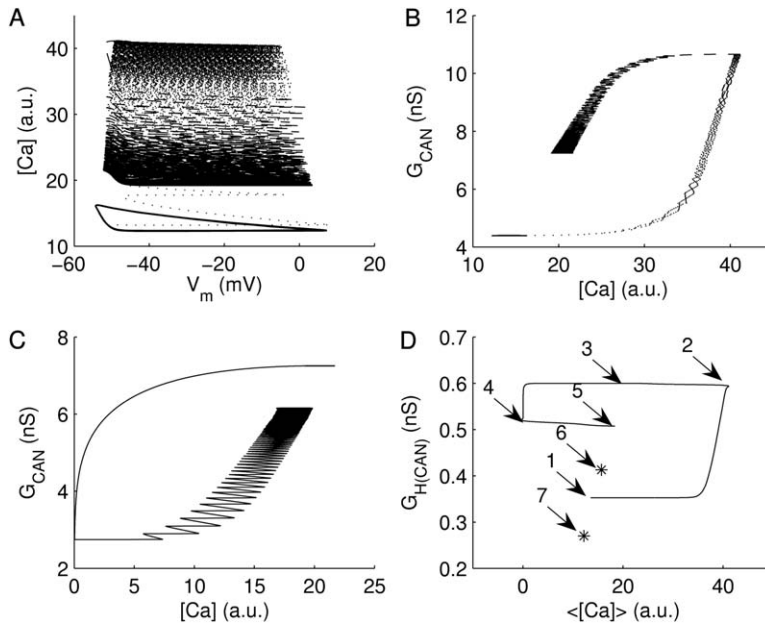


Figure 7. Phase Plane Plot of Model Data
 (A) Calcium concentration versus soma membrane potential during depolarizing current injection for time interval 22–43 s of Figure 6 around (C). Lower closed orbit indicates stable starting level. Dark region above this around 20 units of $[Ca^{2+}]$ indicates ending stable level. During the depolarizing current injection the orbit is brought up to around 40 units. After the end of the current injection, the orbit gradually approaches the ending closed orbit.
 (B) Conductance of cationic current versus calcium concentration. Time and line marks as in (A).
 (C) Conductance of cationic current versus calcium concentration for hyperpolarizing current injection for time interval 46–68 s of Figure 6 around (D).
 (D) Activation of high conductance state of cationic current versus time average (low-pass filtered) calcium concentration. Time interval combining periods from (A) and (C). (1) Start of a depolarizing pulse from a stable level, (2) end of pulse, (3) establishment of a new higher stable level, (4) end of subsequent hyperpolarizing pulse, (5) new lower stable level. (6) and (7) indicate a second and third lower stable level at time point 100 and 115 s of Figure 6. Note how the location of stable levels indicate existence of an isocline.

that these other systems also involve cellular mechanisms of the kind discussed here.

These mechanisms give an EC layer V neuron the properties of an integrator, summing input activity in a continuous manner over time. These mechanisms could allow integration of input to EC from the presubicular and postsubicular cortices (van Haeften et al., 2000), which contain cells that display persistent firing encoding head direction (Taube et al., 1990). Howard et al. (2005) showed that integration of head direction input enables the system to obtain high precision in a spatial location estimate and could contribute to trajectory encoding by EC cells (Frank et al., 2000). The maintenance of graded levels over time could allow a continuum of activity that is necessary for the accuracy of path integration (Fuhs et al., 2005). The mechanism could also contribute to grid cell firing (Hafting et al., 2005). In primates, these effects could contribute to persistent firing in parahippocampal regions for allocentric position of the space being viewed (Georges-Francois et al., 1999).

More generally, graded firing provides a potential mechanism for parametric working memory, maintaining memory for stimuli varying along continuous dimensions, such as somatosensory vibration frequency (Romo et al., 1999) or eye position (Robinson, 1972). Persistent spiking in the absence of synaptic transmission provides a mechanism for maintaining information about novel stimuli, for which prior synaptic representations have not been formed. This could underlie EC activity shown during delayed matching performance for novel stimuli, in contrast to prefrontal activity during delayed matching for familiar stimuli (Stern et al., 2001). Cholinergic modulation is necessary for this persistent spiking, and cholinergic blockade reduces sustained activity recorded in EC during the delay period of a delayed matching task (Schon et al., 2005). Stable graded

firing may represent a fundamental aspect of the function of neuronal networks.

Experimental Procedures

Experimental protocols were approved by the McGill University Animal Care committee and were in compliance with guidelines of the Canadian Council on Animal Care. Procedures for intracellular recording in slices were described in detail in Egorov et al. (2002). In the present study, 30 neurons from layer V of entorhinal cortex were recorded intracellularly using sharp microelectrode techniques at $34^{\circ}\text{C} \pm 1^{\circ}\text{C}$. Because the muscarinic phenomena studied did not desensitize, in most cases (20 out of 30) the neurons were initially impaled in the presence of carbachol (CCh) ($10 \mu\text{M}$). The resting membrane potential of the neurons was $-67.6 \pm 2.4 \text{ mV}$ (mean \pm SD) in control Ringer's solution ($n = 10$) and $-65.1 \pm 2.8 \text{ mV}$ in the presence of CCh ($n = 20$). All recordings were performed during block of glutamatergic and GABA-mediated neurotransmission with kynurenic acid (2 mM) and picrotoxin ($100 \mu\text{M}$). In CPA experiments, because CPA acts by preventing refilling of intracellular calcium stores (Seidler et al., 1989), the solution containing CPA ($50 \mu\text{M}$) was superfused for at least 30 min prior to application of CCh to give the stores time to deplete. By itself CPA caused a small reduction in the AHP (reduction in the peak of the AHP was $-17\% \pm 5\%$; tested for five neurons, Figures 2A1, 2A2, and inset of 2A2), which may be due to a small contribution by Ca^{2+} stores toward activation of the Ca^{2+} -activated K^{+} channels that underlie AHP. However, in these conditions, we still observed graded persistent activity following application of CCh. All the chemicals were purchased from Sigma, except CPA, which was from Tocris and Calbiochem, and thapsigargin from Tocris. CPA, thapsigargin, and 4-aminopyridine (4-AP) were applied from stock solutions made in DMSO so that the final concentration of DMSO in Ringer's solution was 0.1%. Electrophysiological data were analyzed using Clampfit 9.0 (Axon Inst.) and Origin 6.0 (Microcal) software packages.

Biophysical simulations were developed using the GENESIS simulation package (Bower and Beeman, 1995). The method for numerical solution to differential equations was a modified Crank-Nicholson (Hines, 1984). A time step of $50 \mu\text{s}$ was used for the simulations (tests using $25 \mu\text{s}$ did not qualitatively change simulation results). Simulation results were analyzed using Matlab 7. Graded firing rates were simulated in a compartmental model of an

entorhinal cortex layer V principal neuron based on a previously published model of the pyramidal-like cell of EC layer II (Fransén et al., 2002). Further details of model parameters are given in the Supplementary methods.

Biochemical Pathway

Experiments indicate involvement of intracellular calcium from high-threshold calcium channels, and activation of a cationic current (Egorov et al., 2002). The full signaling mechanism from intracellular calcium to cationic current is unknown. This section describes the proposed biochemical pathways added to our previous model (Fransén et al., 2002) to give the graded properties of firing. This biochemical pathway is depicted in Figure 4A.

The influx of calcium through the high-threshold calcium channel Ca_L changes intracellular calcium concentration $[Ca]_{PD}$, which is regulated through pumping and buffering processes modeled according to Traub et al. (1991) and McCormick and Huguenard (1992). $[Ca]_{PD}$ has a linear rise of Ca^{2+} proportional to the Ca_L current and a time constant. The time constant of cytosolic Ca^{2+} for entorhinal layer II stellate cells and layer III pyramidal cells is on the order of 5 s (Gloveli et al., 1999), comparable to Ca^{2+} diffusion simulations of a cell of comparable size (Yamada et al., 1989), where a time constant of around 5 s was found for the core volume. However, to represent Ca^{2+} in a volume closer to the membrane, we used a shorter time constant of 250 ms, in agreement with Yamada et al. (1989). Thus, the slow kinetics of our system are not primarily determined by the time constant of the Ca^{2+} concentration. Instead, it arises from the regulation of I_{CAN} by the intracellular calcium $[Ca]_{CAN}$ as well as by the channel kinetics of I_{CAN} itself, symbolized by the Hodgkin-Huxley-type gates between open (O) and closed (C) state.

$[Ca]_{PD}$ affects two pathways:

(1) High calcium pathway: P. When the calcium concentration $[Ca]_{PD}$ crosses a transition point, it can increase I_{CAN} current via production of a compound X increasing the concentration $[X]$. The product X controls the balance between hypothetical kinases and phosphatases that in turn controls the balance between a phosphorylated state (H) and an unphosphorylated state (L) of the I_{CAN} channel. An increase in $[X]$ causes a fine-grained increase in the number of channels I_{CAN} in a high conductance state, thereby causing a graded increase in firing frequency. This pathway operates only when $[Ca]_{PD}$ is above the transition point $[Ca]_{THP} = 20$. The flux of X production

$$\begin{aligned} \phi_P &= d_P \times ([Ca]_{PD} - [Ca]_{THP}) \text{ for } [Ca]_{PD} \geq [Ca]_{THP} \\ \phi_P &= 0 \text{ otherwise} \\ d_P &= 0.00015, [X] \leq 100 \end{aligned}$$

(2) Low calcium pathway: D. When the calcium concentration $[Ca]_{PD}$ falls below a transition point, it can decrease I_{CAN} current via breakdown of compound X and reduction in concentration $[X]$, $[X] \geq 0$. This pathway operates only when $[Ca]_{PD}$ is below a transition point $[Ca]_{THD} = 5$. The flux of X removal

$$\begin{aligned} \phi_D &= d_D \times ([Ca]_{PD} - [Ca]_{THD}) \text{ for } [Ca]_{PD} < [Ca]_{THD} \\ \phi_D &= 0 \text{ otherwise} \\ d_D &= 0.00005 \text{ and } [Ca]_{THD} < [Ca]_{THP} \end{aligned}$$

A decrease in $[X]$ causes a decrease in the number of individual I_{CAN} channels in a high conductance state and thereby causes a graded decrease in firing frequency. Importantly, in the interval of $[Ca]_{PD}$ between $[Ca]_{THD}$ and $[Ca]_{THP}$, there is no change in $[X]$. This allows the graded levels to remain stable despite small variations (or brief large-amplitude changes) in membrane potential and/or variations in intracellular calcium concentration. Therefore, the graded levels only change when there are large-scale changes in $[Ca]_{PD}$ passing either transition point.

As noted above, the concentration $[X]$ regulates the conductance of I_{CAN} . This was implemented in the model by changing the effective CAN channel current dependent on the level of $[X]$. This describes the transition between the channel state producing a low charge transfer to the state producing a high charge transfer and is meant to encompass processes such as changes in single-channel conductance or channel open time. Any single channel is either in its high or low conductance state. The total conductance of the ion

channel $G_{tot} = g_L \times N_L + g_H \times N_H$. When N_x are large numbers, transitions appear graded (Lisman and Goldring, 1988).

The low and high conductance state dynamics $z = z([X])$ are modeled similarly to the calcium dependent K-current in Traub et al. (1991). The sensitivity to compound X is described by:

$$\begin{aligned} \alpha_z([X]) &= \min(0.015 \times [X], 1.5) \\ \beta_z &= 1.0 \\ \text{gate exponent} &= 1 \end{aligned}$$

z , which is normalized between 0 and 1, is the degree of phosphorylation where 0 represents all CAN channels in the low state and 1 represents the case where the maximal possible number of CAN channels are in the high state.

The conductance of I_{CAN} depends on $[Ca]_{CAN}$, as described in Fransén et al. (2002), see Figure 4A, dashed pathway. The CAN current open and closed gating $y = y([Ca]_{CAN})$ was similarly described by:

$$\begin{aligned} \alpha_m([Ca^{2+}]) &= \min(0.006 \times [Ca^{2+}], 3.0) \\ \beta_m &= 1.0 \\ \text{gate exponent} &= 1 \end{aligned}$$

The additional conductivity of the high conductance state compared to the low conductance state (i.e., the net increase) was added to the maximal conductance of I_{CAN} of the low conductance state associated with its calcium sensitivity: $G_{tot} = G_{CAN} \times y + G_{mod} \times z$, $G_{mod} = 3.7 \times 10^{-8}$ is the scaling constant for the modification z ; G_{CAN} is the maximal conductance of the low state; G_{tot} is the maximal conductance of I_{CAN} at the current level of $[X]$ and $[Ca^{2+}]$.

The pathway model components should not be studied in isolation; they only have a meaning as a whole and do not necessarily by themselves correspond to specific parts of the biochemical pathway. The order of the components does likewise not necessarily correspond to any order in the real system. The gating was modeled according to a first-order scheme (like an equilibrium reaction or like the gating of an H-H channel). We have used a linear model for I_{CAN} , as we presently cannot separate the kinetics of the different components in the pathway, due to insufficient experimental data. An alternative could have been a second-order scheme of an enzyme-type reaction for the modification of I_{CAN} , yielding a hyperbolic system. With regard to localization of functional components on the soma or dendrites, we have used a somatic localization for the model and results presented. Simulations using a dendritic localization (data not shown) produced similar results.

Supplemental Data

The Supplemental Data for this article can be found online at <http://www.neuron.org/cgi/content/full/49/5/735/DC1/>.

Acknowledgments

In memory of Professor Angel A. Alonso, who died July 6, 2005. This work was supported by the Swedish research council 240-00023-061 to E.F., the CIHR to B.T. and A.A., the DFG (SFB 636/A5) and IHNA RAS to A.V.E., and NIH NIMH61492, NIMH60013, NIDA16454 (part of the CRCNS program), and NSF SLC SBE 0354378 to M.H. We thank Pål Westermark and Avrama Blackwell for discussions on modeling of biochemical pathways.

Received: May 9, 2005

Revised: August 4, 2005

Accepted: January 25, 2006

Published: March 1, 2006

References

- Amit, D.J., and Brunel, N. (1997). Model of global spontaneous activity and local structured activity during delay periods in the cerebral cortex. *Cereb. Cortex* 7, 237–252.
- Bower, J.M., and Beeman, D. (1995). *The Book of GENESIS: Exploring Realistic Neural Models with the GENeral NEural Simulation System* (New York: Springer-Verlag).

- Brody, C.D., Romo, R., and Kepecs, A. (2003). Basic mechanisms for graded persistent activity: discrete attractors, continuous attractors, and dynamic representations. *Curr. Opin. Neurobiol.* *13*, 204–211.
- Camperi, M., and Wang, X.J. (1998). A model of visuospatial working memory in prefrontal cortex: recurrent network and cellular bistability. *J. Comput. Neurosci.* *5*, 383–405.
- Cannon, S.C., Robinson, D.A., and Shamma, S. (1983). A proposed neural network for the integrator of the oculomotor system. *Biol. Cybern.* *49*, 127–136.
- Cho, K., Aggleton, J.P., Brown, M.W., and Bashir, Z.I. (2001). An experimental test of the role of postsynaptic calcium levels in determining synaptic strength using perirhinal cortex of rat. *J. Physiol.* *532*, 459–466.
- Compte, A., Brunel, N., Goldman-Rakic, P.S., and Wang, X.J. (2000). Synaptic mechanisms and network dynamics underlying spatial working memory in a cortical network model. *Cereb. Cortex* *10*, 910–923.
- Connors, B.W. (2002). Single-neuron mnemonics. *Nature* *420*, 133–134.
- Durstewitz, D. (2003). Self-organizing neural integrator predicts interval times through climbing activity. *J. Neurosci.* *23*, 5342–5353.
- Egorov, A.V., Hamam, B.N., Fransén, E., Hasselmo, M.E., and Alonso, A.A. (2002). Graded persistent activity in entorhinal cortex neurons. *Nature* *420*, 173–178.
- Frank, L.M., and Brown, E.N. (2003). Persistent activity and memory in the entorhinal cortex. *Trends Neurosci.* *26*, 400–401.
- Frank, L.M., Brown, E.N., and Wilson, M. (2000). Trajectory encoding in the hippocampus and entorhinal cortex. *Neuron* *27*, 169–178.
- Fransén, E., and Lansner, A. (1995). Low spiking rates in a population of mutually exciting pyramidal cells. *Network* *6*, 271–288.
- Fransén, E., and Lansner, A. (1998). A model of cortical associative memory based on a horizontal network of connected columns. *Network* *9*, 235–264.
- Fransén, E., Alonso, A.A., and Hasselmo, M.E. (2002). Simulations of the role of the muscarinic-activated calcium-sensitive nonspecific cation current INCM in entorhinal neuronal activity during delayed matching tasks. *J. Neurosci.* *22*, 1081–1097.
- Fuhs, M.C., Vanrhoads, S.R., Casale, A.E., McNaughton, B., and Touretzky, D.S. (2005). Influence of path integration versus environmental orientation on place cell remapping between visually identical environments. *J. Neurophysiol.* *94*, 2603–2616.
- Georges-Francois, P., Rolls, E.T., and Robertson, R.G. (1999). Spatial view cells in the primate hippocampus: allocentric view not head direction or eye position or place. *Cereb. Cortex* *9*, 197–212.
- Gloveli, T., Egorov, A.V., Schmitz, D., Heinemann, U., and Muller, W. (1999). Carbachol-induced changes in excitability and $[Ca^{2+}]_i$ signaling in projection cells of medial entorhinal cortex layers II and III. *Eur. J. Neurosci.* *11*, 3626–3636.
- Hafting, T., Fyhn, M., Molden, S., Moser, M.B., and Moser, E.I. (2005). Microstructure of a spatial map in the entorhinal cortex. *Nature* *436*, 801–806.
- Heckman, C.J., Lee, R.H., and Brownstone, R.M. (2003). Hyperexcitable dendrites in motoneurons and their neuromodulatory control during motor behaviour. *Trends Neurosci.* *26*, 688–695.
- Hines, M. (1984). Efficient computation of branched nerve equations. *Int. J. Biomed. Comput.* *15*, 69–76.
- Howard, M.W., Fotedar, M.S., Datey, A.V., and Hasselmo, M.E. (2005). The temporal context model in spatial navigation and relational learning: Toward a common explanation of medial temporal lobe function across domains. *Psychol. Rev.* *112*, 75–116.
- Inoue, R., Waniishi, Y., Yamada, K., and Ito, Y. (1994). A possible role of tyrosine kinases in the regulation of muscarinic receptor-activated cation channels in guinea pig ileum. *Biochem. Biophys. Res. Commun.* *203*, 1392–1397.
- Klink, R., and Alonso, A. (1997). Ionic mechanisms of muscarinic depolarization in entorhinal cortex layer II neurons. *J. Neurophysiol.* *77*, 1829–1843.
- Koene, R.A., Gorchetchnikov, A., Cannon, R.C., and Hasselmo, M.E. (2003). Modeling goal-directed spatial navigation in the rat based on physiological data from the hippocampal formation. *Neural Netw.* *16*, 577–584.
- Koulakov, A.A., Raghavachari, S., Kepecs, A., and Lisman, J.E. (2002). Model for a robust neural integrator. *Nat. Neurosci.* *5*, 775–782.
- Lisman, J.E. (2001). Three Ca^{2+} levels affect plasticity differently: the LTP zone, the LTD zone and no man's land. *J. Physiol.* *532*, 285.
- Lisman, J. (1994). The CaM kinase II hypothesis for the storage of synaptic memory. *Trends Neurosci.* *17*, 406–412.
- Lisman, J.E., and Goldring, M.A. (1988). Feasibility of long-term storage of graded information by the Ca^{2+} /calmodulin-dependent protein kinase molecules of the postsynaptic density. *Proc. Natl. Acad. Sci. USA* *85*, 5320–5324.
- Lisman, J.E., and Idiart, M.A. (1995). Storage of 7 ± 2 short-term memories in oscillatory subcycles. *Science* *267*, 1512–1515.
- Loewenstein, Y., and Sompolinsky, H. (2003). Temporal integration by calcium dynamics in a model neuron. *Nat. Neurosci.* *6*, 961–967.
- Major, G., and Tank, D. (2004). Persistent neural activity: Prevalence and mechanisms. *Curr. Opin. Neurobiol.* *14*, 675–684.
- McCormick, D.A., and Huguenard, J.R. (1992). A model of the electrophysiological properties of thalamocortical relay neurons. *J. Neurophysiol.* *68*, 1384–1400.
- Miller, P., Brody, C.D., Romo, R., and Wang, X.J. (2003). A recurrent network model of somatosensory parametric working memory in the prefrontal cortex. *Cereb. Cortex* *13*, 1208–1218.
- Okamoto, H., and Ichikawa, K. (1994). Model for an enzymatic reaction-diffusion system realizing storage of graded information. *Phys. Rev. E Stat. Phys. Plasmas Fluids Relat. Interdiscip. Topics* *50*, 1704–1707.
- Robinson, D.A. (1972). On the nature of visual-oculomotor connections. *Invest. Ophthalmol.* *11*, 497–503.
- Romo, R., Brody, C.D., Hernandez, A., and Lemus, L. (1999). Neuronal correlates of parametric working memory in the prefrontal cortex. *Nature* *399*, 470–473.
- Runyan, J.D., Moore, A.N., and Dash, P.K. (2005). A role for prefrontal calcium-sensitive protein phosphatase and kinase activities in working memory. *Learn. Mem.* *12*, 103–110.
- Schon, K., Atri, A., Hasselmo, M.E., Tricarico, M.D., LoPresti, M.L., and Stern, C.E. (2005). Scopolamine reduces persistent activity related to long-term encoding in the parahippocampal gyrus during delayed matching in humans. *J. Neurosci.* *25*, 9112–9123.
- Seidler, N.W., Jona, I., Vegh, M., and Martonosi, A. (1989). Cyclopiazonic acid is a specific inhibitor of the Ca^{2+} -ATPase of sarcoplasmic reticulum. *J. Biol. Chem.* *264*, 17816–17823.
- Seung, H.S., Lee, D.D., Reis, B.Y., and Tank, D.W. (2000). Stability of the memory of eye position in a recurrent network of conductance-based model neurons. *Neuron* *26*, 259–271.
- Shalinsky, M.H., Magistretti, J., Ma, L., and Alonso, A.A. (2002). Muscarinic activation of a cation current and associated current noise in entorhinal-cortex layer-II neurons. *J. Neurophysiol.* *88*, 1197–1211.
- Stern, C.E., Sherman, S.J., Kirchoff, B.A., and Hasselmo, M.E. (2001). Medial temporal and prefrontal contributions to working memory tasks with novel and familiar stimuli. *Hippocampus* *11*, 337–346.
- Taube, J.S., and Bassett, J.P. (2003). Persistent neural activity in head direction cells. *Cereb. Cortex* *13*, 1162–1172.
- Taube, J.S., Muller, R.U., and Ranck, J.B. (1990). Head-direction cells recorded from the postsubiculum in freely moving rats. I. Description and quantitative analysis. *J. Neurosci.* *10*, 420–435.
- Teramae, J.-N., and Fukai, T. (2005). A cellular mechanism for graded persistent activity in a model neuron and its implications in working memory. *J. Comput. Neurosci.* *18*, 105–121.
- Traub, R.D., Wong, R.K.S., Miles, R., and Michelson, H. (1991). A model of a CA3 pyramidal neuron incorporating voltage-clamp data on intrinsic conductances. *J. Neurophysiol.* *66*, 635–650.

van Haeften, T., Wouterlood, F.G., and Witter, M.P. (2000). Presubicular input to the dendrites of layer-V entorhinal neurons in the rat. *Ann. N Y Acad. Sci.* 911, 471–473.

Walters, R.J., Kramer, R.H., and Nawy, S. (1998). Regulation of cGMP-dependent current in On bipolar cells by calcium/calmodulin-dependent kinase. *Vis. Neurosci.* 15, 257–261.

Wang, S.S., and Major, G. (2003). Integrating over time with dendritic wave-fronts. *Nat. Neurosci.* 6, 906–908.

Yamada, W., Koch, C., and Adams, P. (1989). Multiple channels and calcium dynamics. In *Methods in Neuronal Modeling. From Synapses to Networks*, C. Koch and I. Segev, eds. (Cambridge, MA: MIT Press), pp. 97–134.